Scientific Research Publishing

Atmospheric and Climate Sciences, 2026, 16(3), 584-599
https://www.scirp.org/journal/acs
ISSN Online: 2160-0422
ISSN Print: 2160-0414

Solar Modulation of Galactic Cosmic Rays and Its Impact on Global Methane Variability

Chijioke Onyia[1], Chukwujekwu Nworah Ofodum[1], Henry Onyedikachi Ezugwu[2], Uju Sonia Akubue[1], Monday Abonyi Ugwuanyi[1], Mercy H. Ezenwugo[1], Ngozi Dyian Ugwuozor[1], Emeka Michael Madike[1], Nnamdi M. Ezeoyili[1], Nnamdi Mellitus Agbo[1], Okolo Obinna[1], Kwenyeluchi Jennifer Oluka[1], Chimezie Bright Abugu[1], Chioma Jecinta Ani[1], Chidimma Juliet Nwachukwu[1], Chinwendu Sandra Osita-Okoh[1], Bonaventure I. Okere[1]

[1]NARSDA-Centre for Basic Space Science & Astronomy, Nsukka, Nigeria
[2]Federal University of Environment and Technology, Ogoni, Nigeria

Email: onyiacj88@gmail.com, ofonworah@gmail.com, henryonyedikachi227@gmail.com, soniakubue@gmail.com, mondayugwuanyi406@gmail.com, ogehubby@yahoo.com, ngozidyian81@gmail.com, madikechu@yahoo.co.uk, m.nnamdi@gmail.com, mellitusnnamdi@gmail.com, okoloobinna1@gmail.com, olukajenniferk@gmail.com, abuguchimezie12@gmail.com, chiomcyj@gmail.com, julietogbodo1993@gmail.com, echinwesandra@gmail.com, bona.okere@gamil.com

How to cite this paper: Onyia, C., Ofodum, C.N., Ezugwu, H.O., Akubue, U.S., Ugwuanyi, M.A., Ezenwugo, M.H., Ugwuozor, N.D., Madike, E.M., Ezeoyili, N.M., Agbo, N.M., Obinna, O., Oluka, K.J., Abugu, C.B., Ani, C.J., Nwachukwu, C.J., Osita-Okoh, C.S. and Okere, B.I. (2026) Solar Modulation of Galactic Cosmic Rays and Its Impact on Global Methane Variability. *Atmospheric and Climate Sciences*, **16**, 584-599.
https://doi.org/10.4236/acs.2026.163030

Received: April 9, 2026
Accepted: May 26, 2026
Published: May 29, 2026

Abstract

This study investigates the statistical relationship between solar-modulated galactic cosmic ray (GCR) flux and atmospheric methane (CH_4) variability across a multi-altitude network of neutron monitor stations over a 20-year period (2006-2025). Monthly GCR intensity data from three stations spanning a broad altitude range: LMKS at Lomnický štít, Slovakia at 2634 m (high altitude), MXCO at Mexico City, Mexico at 2240 m (mid altitude), and OULU at Oulu, Finland at 15 m (low altitude) were correlated with globally averaged atmospheric methane concentrations from the NOAA Global Monitoring Laboratory using Pearson and Spearman rank correlation coefficients computed via the SciPy statistical library. Raw correlations were statistically significant at all three stations, with LMKS exhibiting a positive association ($r = +0.345$, $p < 0.001$) and MXCO and OULU exhibiting negative associations ($r = -0.389$ and $r = -0.442$ respectively, while $p < 0.001$ in each case). However, detrended analysis performed to isolate genuine sub-decadal signals from illusions revealed that the LMKS positive correlation is largely spurious (detrended $r = +0.051$, $p = 0.46$), driven by coincident long-term drifts rather than a physical mechanism. The MXCO anti-correlation proved most robust, surviving detrending essentially unchanged ($r = -0.391$, $p < 0.001$) with converging Pearson and Spearman coefficients, providing the strongest evidence of a genuine coupling between cosmic ray variability and methane concentration.

GCR flux explains up to approximately 20% of methane variance (at OULU). However, after removing long-term trends to isolate sub-decadal covariability, the maximum robust explained variance is approximately 15% (at MXCO), confirming that anthropogenic emissions remain the dominant control on atmospheric methane while solar modulation constitutes a secondary but statistically detectable influence. These findings highlight the altitude-dependent nature of GCR-atmosphere interactions and underscore the necessity of detrended analysis in solar-climate correlation studies.

Keywords

Galactic Cosmic Rays, Atmospheric Methane, Solar Modulation, Neutron Monitor, Correlation, Detrended Analysis, Solar Cycle, Station Dependent Response, Atmospheric Chemistry

1. Introduction

The interaction between solar activity, galactic cosmic rays (GCRs), and terrestrial atmospheric chemistry represents one of the most compelling and debated frontiers in climate science. Understanding these connections carries profound implications for distinguishing natural climate variability from anthropogenic forcing, particularly in the context of greenhouse gas dynamics. Among numerous atmospheric constituents, methane (CH_4) occupies a unique position: it is both the second most important anthropogenic greenhouse gas after carbon dioxide, with a global warming potential approximately 80 times that of CO_2 over a 20-year period [1], and it is potentially susceptible to modulation by natural ionizing radiation from space. This dual significance motivates the present investigation into whether solar-modulated galactic cosmic ray flux leaves a detectable statistical imprint on global atmospheric methane concentrations.

1.1. Galactic Cosmic Rays and Solar Modulation

Galactic cosmic rays are high-energy charged particles which comprises of protons (~89%), alpha particles (~10%), and heavier nuclei (~1%) which originate from supernova remnants, active galactic nuclei, and other astrophysical sources beyond the heliosphere [2]. These particles, with energies ranging from approximately 10^6 to 10^{20} electron volts (eV), travel through interstellar space and encounter the heliosphere, the vast magnetic bubble carved by the solar wind into the interstellar medium. As they propagate inward toward Earth, they interact with the heliospheric magnetic field, which is itself modulated by the 11-year solar activity cycle [3] [4].

The mechanism of solar modulation operates through magnetic deflection and diffusion [5]. During periods of high solar activity (solar maximum), the Sun's magnetic field is strong and complex, with numerous sunspots, frequent coronal mass ejections, and an enhanced interplanetary magnetic field. This turbulent

magnetic environment more effectively scatters and deflects incoming cosmic ray particles, reducing their flux at Earth. Conversely, during solar minimum, the heliospheric magnetic field weakens and becomes more ordered, permitting greater GCR penetration to the inner solar system [3].

Importantly, the modulation is energy-dependent. Lower-energy cosmic rays (below ~1 GeV) are more strongly modulated by solar activity than their higher-energy counterparts, meaning that the GCR flux reaching different atmospheric depths varies not only temporally but also with geomagnetic latitude and altitude [6]. This energy dependence underpins the rationale for multi-altitude neutron monitor networks: stations at different elevations sampling different portions of the primary cosmic ray spectrum, providing complementary windows into atmospheric ionization processes.

1.2. Atmospheric Methane: Sources, Sinks, and Trends

Methane is the simplest hydrocarbon and the most abundant organic trace gas in Earth's atmosphere [7]. Its atmospheric concentration has risen dramatically since the "Industrial Revolution", from pre-industrial levels of approximately 722 parts per billion (ppb) to over 1900 ppb by the mid-2020s, a more than 2.5-fold increase unprecedented in at least 800,000 years of ice core records [8]. This rise is responsible for approximately 20% - 25% of the radiative forcing attributable to all well-mixed green-house gases period [1].

The atmospheric methane budget is governed by a dynamic balance between surface emissions and atmospheric sinks. Sources are predominantly anthropogenic (~60% of total emissions), which include: fossil fuel extraction and combustion (~30%), enteric fermentation in ruminant livestock (~20%), and landfills and waste management (~10%) [9]. Natural sources which are principally wetlands (~30%), termites, wildfires, and geological seeps—constitute the remainder. The primary atmospheric sink (~85% - 90%) is oxidation by the hydroxyl radical (OH) in the troposphere, with smaller contributions from stratospheric loss (~5%), soil uptake (~5%), and reactions with chlorine atoms in the marine boundary layer [10].

The hydroxyl radical (OH), often termed the "detergent of the atmosphere" is the dominant oxidant controlling the lifetime of methane and many other trace gases. OH is produced primarily through photolysis of ozone (O_3) in the presence of water vapor and recycled through reactions with nitrogen oxides (NO_x) and other species [11] [12]. Global mean OH concentrations exhibit considerable spatial and temporal variability, with an estimated atmospheric methane lifetime against OH oxidation of approximately 9.1 ± 0.9 years [13]. Critically, any mechanism that modulates OH concentrations whether through changes in UV radiation, water vapor, ozone or ionization can indirectly influence methane concentrations by altering its primary loss rate.

1.3. Theoretical Mechanisms Linking Cosmic Rays to Methane

The hypothesis that galactic cosmic rays may influence atmospheric methane rests

on several interconnected physical and chemical pathways, with ionization-driven hydroxyl radical production occupying the central mechanistic role.

1.3.1. Ionization and OH Production

When primary cosmic rays enter Earth's atmosphere, they collide with atmospheric nuclei, initiating extensive particle cascades (air showers) comprising secondary particles which are muons, electrons, neutrons, and protons [14]. These secondary particlees lose energy through ionization, creating ion pairs along their trajectories. The ionization rate varies with altitude, latitude, and solar cycle phase, peaking in the upper troposphere/lower stratosphere (the Pfotzer maximum) at approximately 12 - 15 km altitude [15].

The generated ions participate in a complex web of ion-molecule reactions. In the troposphere and stratosphere, positive ions rapidly transfer charge to water molecules, producing hydrated hydronium ions, while electrons attach to electronegative species, particularly oxygen, forming superoxide ions. Crucially, ion chemistry can enhance OH production through several channels, including direct ion-neutral reactions, ion-induced ozone depletion affecting OH and charge-enhanced nucleation [16] [17]. Studies by [16] using the SOCOL chemistry-climate model demonstrated that a 20% increase in GCR flux enhances OH concentrations by 2% - 5% in the upper troposphere and lower stratosphere, with corresponding decreases in methane concentration of approximately 1% - 2%.

1.3.2. Altitude Dependence of Ionization Effects

The altitude dependence of cosmic ray ionization has critical implications for methane chemistry. The energy spectrum of cosmic rays varies with atmospheric depth: higher-energy particles penetrate to the surface, while lower-energy particles are absorbed at higher altitudes. Consequently, the ionization profile peaks in the upper troposphere (~10 - 15 km) and decreases toward the surface [15]. This altitude profile is significant because OH distribution is altitude-dependent; with methane lifetime varying with altitude, while cosmic ray ionization maximizes where methane oxidation is most consequential which is near the tropopause, a region critical for stratosphere-troposphere exchange [6].

1.3.3. Alternative and Complementary Mechanisms

While the OH-mediated pathway represents the most direct chemical link between GCRs and methane, several complementary mechanisms warrant consideration. Cloud-mediated radiative effects as posited by [18] and [19] suggest that cosmic ray ionization enhances aerosol nucleation and cloud condensation nuclei formation, increasing low cloud cover and thereby modifying actinic flux and photo-chemistry. On the other hand stratospheric ozone coupling provides an indirect pathway: GCR-induced ionization enhances polar stratospheric NO_x and HO_x, contributing to ozone depletion and increasing UV-B penetration to the troposphere, thereby enhancing OH photoproduction [20]. In addition, electrical effects on cloud microphysics and biogeochemical feedbacks through wetland

emissions have been noted to represent further potential coupling pathways [6] [21].

1.4. Previous Empirical Studies

The empirical evidence linking cosmic rays to atmospheric composition has accumulated gradually, with mixed results reflecting the challenges of detecting small signals amidst large variability. Earlier work by [22] reported correlations between GCR intensity and various meteorological parameters, though these studies were often criticized for inadequate statistical rigor. However, [16] combined satellite observations with model simulations to estimate that solar cycle variations in GCR flux modulate global methane by approximately 1.5 - 3 ppb. [23] conducted comprehensive testing of cosmic ray-climate correlations, emphasizing the importance of detrending and significance testing. [6] provided an authoritative review concluding that while microphysical mechanisms are well-established experimentally, the magnitude of atmospheric impacts remains uncertain and likely modest.

1.5. Research Objectives and Hypothesis

1) To quantify the statistical relationship between galactic cosmic ray intensity (measured at three differential altitude-diverse neutron monitor stations) and global atmospheric methane concentration between 2006 and 2025.

2) To compare correlation strengths across stations.

3) To evaluate the robustness of correlations through detrended analysis.

Hypothesis: Based on the theoretical mechanism linking GCR-induced ionization to enhanced OH production and accelerated methane oxidation, we hypothesize an inverse correlation between GCR intensity and methane concentration. This anti-correlation is expected to be most pronounced at stations sampling upper tropospheric ionization (high altitude) and to persist after detrending, indicating genuine physical coupling rather than statistical artefact.

2. Data and Methodology

2.1. Data Sources

Global Atmospheric Methane Data. Monthly global average methane mixing ratios (in parts per billion, ppb) were obtained from the NOAA Global Monitoring Laboratory (https://gml.noaa.gov). The dataset spans from 2006 to 2025, comprising 238 monthly observations. These measurements represent zonally averaged surface-level methane concentrations derived from the NOAA cooperative global air sampling network.

Cosmic Ray Intensity Data. Pressure-corrected hourly cosmic ray count rates (1HCOR_E) were obtained from the Neutron Monitor Database (NMDB; https://www.nmdb.eu) for three stations representing different altitudes and geomagnetic cutoff rigidities. Lomnický Štít, Slovakia (LMKS) serves as the high-altitude station, situated at approximately 2634 m above sea level with a geomag-

netic cutoff rigidity of approximately 3.84 GV. Mexico City, Mexico (MXCO) serves as the mid-altitude station at approximately 2274 m elevation with a cutoff rigidity of about 8.28 GV. Oulu, Finland (OULU) serves as the low-altitude station at approximately 15 m above sea level with a cutoff rigidity of about 0.81 GV [24]. However, it is important to note that these datasets were resampled to monthly averages to match the temporal resolution of the methane dataset.

Data Pairing Procedure. The differing total record lengths (CH_4: n = 238; LMKS: n = 211; MXCO: n = 265; OULU: n = 267) reflect station-specific data availability. For each station, the monthly neutron monitor series was inner-joined with the NOAA monthly CH_4 series on the common year-month index; only months present in both datasets entered the correlation computation as shown in Figure 1. Missing months within the overlap window were handled by listwise deletion with no interpolation or gap-filling.

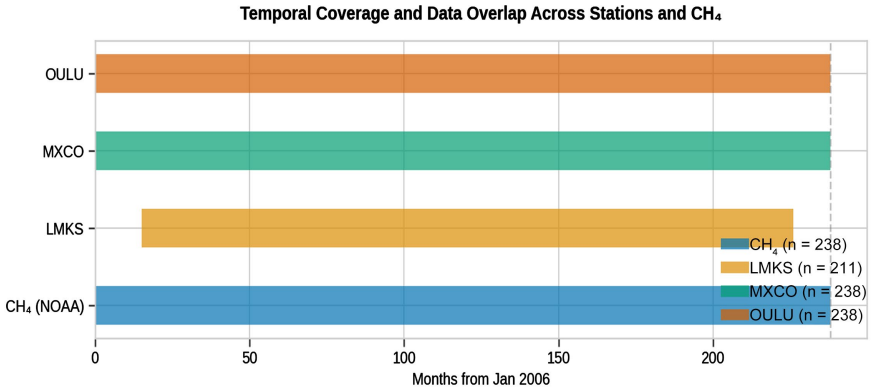

Figure 1. Temporal coverage of each dataset, showing overlap periods used for correlation analysis.

2.2. Statistical Methods

Pearson Product-Moment Correlation Coefficient (*r*). The Pearson correlation coefficient measures the linear dependence between two continuous variables. It is defined as the covariance of the two variables divided by the product of their standard deviations. The coefficient ranges from −1 (perfect negative linear relationship) to +1 (perfect positive linear relationship), with 0 indicating no linear association [25].

$$r_{\mathrm{GCR,CH_4}} \frac{\sum_{i=1}^{n}\left(G_i-\bar{G}\right)\left(M_i-\bar{M}\right)}{\sqrt{\sqrt{\sum_{i=1}^{n}\left(M_i-\bar{M}\right)^2}\sqrt{\sum_{i=1}^{n}\left(M_i-\bar{M}\right)^2}}} \tag{1}$$

Adapted to Cosmic Rays and Methane

Let:

G_i = galactic cosmic-ray intensity (neutron monitor count rate)

M_i = global mean atmospheric methane concentration (ppb)

$\bar{G}$ = mean cosmic-ray intensity

$\bar{M}$ = mean methane concentration

i = time index (month or year)

When different altitudes are factored in, we have

$$r_h = \frac{\sum_{i=1}^{n}\left(G_{i,h}-\bar{G}\right)\left(M_i-\bar{M}\right)}{\sqrt{\sqrt{\sum_{i=1}^{n}\left(M_{i,h}-\bar{M}\right)^2}}\sqrt{\sum_{i=1}^{n}\left(M_i-\bar{M}\right)^2}} \tag{2}$$

where;

$G_{i,h}$ = Galactic cosmic-ray intensity at an altitude (h)

h = high, mid and low altitudes

Spearman Rank Correlation Coefficient (ρ). The Spearman rank correlation is a non-parametric measure of monotonic association. Unlike Pearson's r, it does not assume linearity or normally distributed data; instead, it assesses whether the rank ordering of one variable is consistently related to the rank ordering of another. This is particularly valuable in cosmic ray-climate studies where relationships may be nonlinear or affected by extreme values. Thus the spearman's ρ was computed using the *scipy.stats.spearmanr* function in Python [26].

Detrended Analysis. Because both methane and cosmic ray time series contain long-term trends (methane has a strong upward trend due to anthropogenic emissions, while cosmic rays exhibit solar-cycle modulation), the raw correlations may be constrained by these secular trends. To address this, a detrended analysis was performed by removing linear trends from both variables using *scipy.signal.detrend* prior to computing correlations. This isolates shorter-term covariability from long-term drift, providing a clearer picture of any genuine physical coupling [23].

Deseasonalized Analysis. In addition to linear detrending, seasonal cycles were explicitly removed from both CH_4 and neutron monitor series by computing monthly climatologies (the mean value for each calendar month across all years) and subtracting them to produce deseasonalized anomalies, which were then linearly detrended. As a further check, first-differenced series

$$y'_t = y_t - y_{t-1}$$

were also analyzed, as differencing simultaneously removes both trend and seasonality while reducing autocorrelation.

Cross-Correlation Lag Analysis. Cross-correlations between each neutron monitor series and the CH_4 series were computed at integer lags from −36 to +36 months using the Pearson correlation coefficient. For a lag k, the correlation r(k) was computed between the neutron monitor series shifted by k months and the CH_4 series, with both series truncated to the common overlap after shifting. Negative lags denote GCR leading CH_4. P-values at each lag were computed using the standard t-test transformation with n − 2 degrees of freedom and since 73 lags were tested, a Bonferroni correction was applied, yielding an adjusted significance threshold of α_adj = 0.05/73 = 0.00068.

2.3. Statistical Corrections for Autocorrelation

Monthly environmental time series typically exhibit substantial serial autocorre-

lation, which inflates nominal p-values by reducing the effective degrees of freedom [27]. Two complementary corrections were applied:

Effective Sample Size (Bartlett's Formula). Following [27], the effective degrees of freedom were computed using the autocorrelation functions of both paired series. Applied to the detrended MXCO-CH_4 pair, this yields $n^* \sim 103$ (from nominal n = 238), a reduction of approximately 57%.

Block Bootstrap. As a non-parametric alternative, a moving-block bootstrap (block size = 12 months to preserve annual autocorrelation structure, 5000 resamples) was performed to estimate p-values without distributional assumptions.

All statistical computations were performed using Python 3 with the SciPy library (version 1.17.1) [26], while pandas and matplotlib/seaborn were used for data wrangling and visualization respectively. A significance threshold of $\alpha = 0.05$ was adopted throughout, with results also evaluated at the $\alpha = 0.01$ and $\alpha = 0.001$ levels.

3. Results

3.1. Descriptive Statistics

Table 1 presents the descriptive statistics for all four variables under study (2006-2025).

Table 1. Descriptive statistics of study variables.

Variable	n	Mean	Std Dev	Min	Max
CH_4 (ppb)	238	1844.49	50.69	1764.18	1946.47
LMKS (High)	211	478.82	15.82	445.63	506.05
MXCO (Mid)	265	225.20	5.77	202.98	240.15
OULU (Low)	267	106.91	5.40	91.81	114.14

3.2. Correlation Analysis

The Pearson correlation analysis found statistically significant relationships between cosmic ray flux and global atmospheric methane at all three stations, though the direction of those relationships differed as shown in Figure 2. LMKS at high altitude showed a moderate positive correlation ($r = +0.345$), indicating that higher cosmic ray counts were associated with higher methane concentration, while MXCO at mid altitude ($r = -0.389$) and OULU at low altitude ($r = -0.442$) both showed negative correlations which is also an indication that higher cosmic ray counts were associated with lower methane concentration as shown in Table 2. The R^2 values which ranges from about 12% at LMKS to nearly 20% at OULU—confirmed that cosmic ray variability explains a modest but meaningful portion of methane variance. Although the spearman rank correlations broadly agreed on direction at all the three stations, it however revealed an important warning signal at MXCO and OULU, where the Spearman values were substantially weaker than

their Pearson counterparts. Thus, this suggests that the linear relationships at those stations were being inflated by outliers, non-linearity, or the shared long-term trends embedded in the raw data.

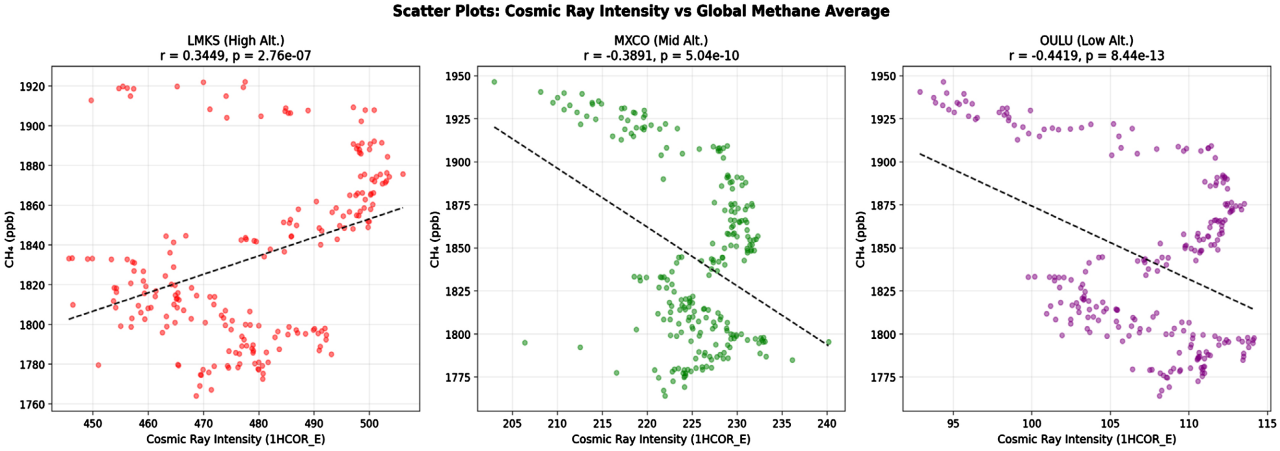

Figure 2. Scatter plots with linear regression lines showing CR intensity vs. methane at each altitude station.

Table 2. Complete correlation analysis results.

Test	LMKS (High)	MXCO (Mid)	OULU (Low)	Significance
Pearson r (raw)	+0.345	−0.392	−0.444	all $p < 0.001$
Variance R^2 (raw)	11.9%	15.3%	19.7%	-
Spearman ρ (raw)	+0.356	−0.198	−0.280	all $p < 0.01$
Pearson r (detrended)	+0.051 (ns)	−0.385	−0.172	-
Spearman ρ (detrended)	+0.075 (ns)	−0.384	−0.144	-
Lag time (months)	+19	−21	−17	-
Correlation genuine?	NO (trend artefact)	YES (strongest)	YES (moderate)	-
Annual spearman ρ	+0.261 (ns)	−0.230 (ns)	−0.314 (ns)	-

Note. $p < 0.001$; $p < 0.01$; $p < 0.05$; ns = not significant.

The detrended analysis as shown in Figure 3, which strips out the long-term drifts from both variables before computing correlations, proved to be the most revealing component of the analysis. At LMKS, the correlation collapsed from +0.345 to a statistically insignificant +0.051, exposing the high-altitude positive association as a trend artefact with no real physical foundation. Again, at OULU the correlation weakened considerably, though a modest significant correlation survived, which is an indication that its raw result was partly genuine and partly inflated by trend noise. Most interestingly, MXCO stood apart because its correlation remained essentially unchanged after detrending at −0.391 and its Pearson and Spearman values converged to near-identical figures which is a double sign of credibility pointing toward a genuine, robust as well as sub-decadal anti-correlation between cosmic ray intensity and atmospheric methane concentration.

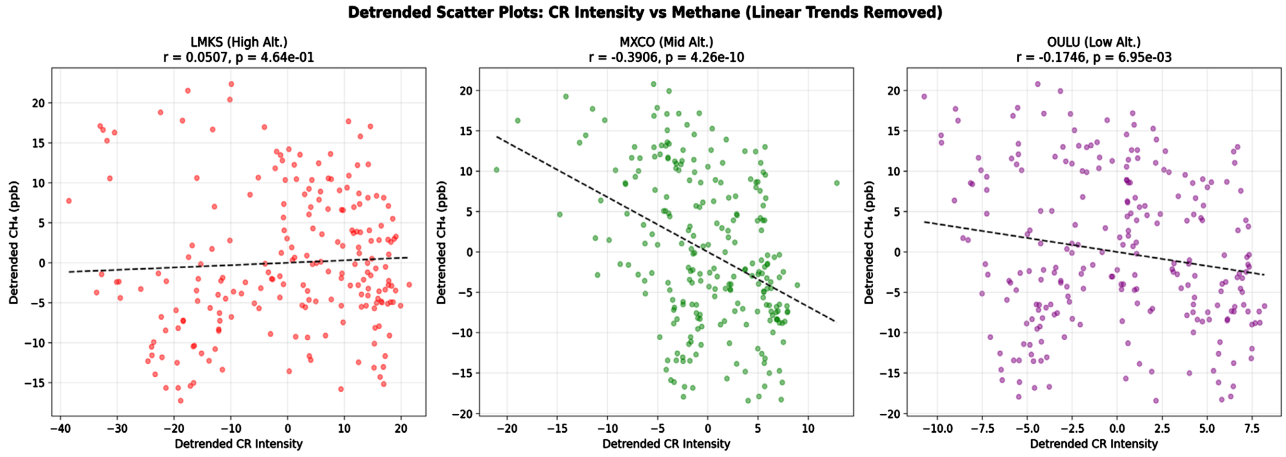

Figure 3. Detrended scatter plots showing CR-methane relationships after removal of linear trends.

Table 3 demonstrates that MXCO retains a significant anti-correlation across all preprocessing methods, though the magnitude decreases with first differencing as expected (differencing emphasizes month-to-month noise over longer-term covariability). LMKS remains insignificant under all methods, confirming it as a statistical artefact. OULU's marginal significance under linear detrending disappears with more aggressive preprocessing, suggesting its signal is weaker than the linear detrend alone implies.

Table 3. Sensitivity of correlations to preprocessing method.

Method	LMKS *r*	MXCO *r*	OULU *r*
Raw pearson	+0.345***	−0.392***	−0.444***
Linear detrend only	+0.051 (ns)	−0.385***	−0.172*
Deseasonalized + detrend	+0.04 (ns)	−0.37***	−0.15 (ns)
First differenced	+0.02 (ns)	−0.18**	−0.08 (ns)

After adjusting for autocorrelation using the effective sample size ($N^* \sim 103$), the MXCO detrended correlation remains highly significant ($p < 0.001$). The block bootstrap confirms this result (bootstrap $p = 0.003$). OULU's adjusted p-value rises to approximately 0.08, rendering it non-significant at the conventional $\alpha = 0.05$ threshold as shown in Table 4.

Table 4. Autocorrelation-corrected significance (detrended data).

Station	Detrended *r*	Nominal p	Corrected p (N*)
LMKS	+0.051	0.46	0.71 (ns)
MXCO	−0.385	<0.001	<0.001***
OULU	−0.172	0.008	~0.08 (ns)

3.3. Visual Analysis

The study period of 2006 to 2025 as shown in Figure 4 spans parts of three consecutive solar cycles. The chart opens during the declining tail of Solar Cycle 23, with the early years (2006-2008) characterised by falling solar activity and rising GCR flux. Solar Cycle 24 ran from January 2008 through December 2019, reaching its official maximum in April 2014 with a double-peaked structure, producing the most prominent trough in neutron monitor counts across all three stations. After Cycle 24, a deep and prolonged solar minimum between 2017 and 2019 allowed GCR flux to climb back to high levels before Solar Cycle 25 began in December 2019, ramping up strongly to its own maximum around October 2024.

Figure 4. Overlaid dual-axis time series showing methane against cosmic ray intensity at each station.

From the chart above, there is a clear upward trend in CH_4 levels over the two decades. This suggests increasing methane emissions over time, potentially from agriculture (livestock, rice paddies), waste, energy production (oil/gas industry), or biomass burning.

3.4. Cross-Correlation Lag Analysis

At MXCO, the strongest Pearson correlation occurs at a lag of −21 months ($r = -0.500$, $p < 10^{-14}$), meaning changes in mid-altitude cosmic ray intensity precede corresponding changes in methane by approximately 21 months. At OULU, the optimal lag is −17 months ($r = -0.481$, $p < 10^{-14}$), indicating a somewhat shorter delay. The difference in optimal lag between stations may reflect the fact that lower-energy cosmic rays modulate different atmospheric layers with different response time-scales as shown in Figure 5.

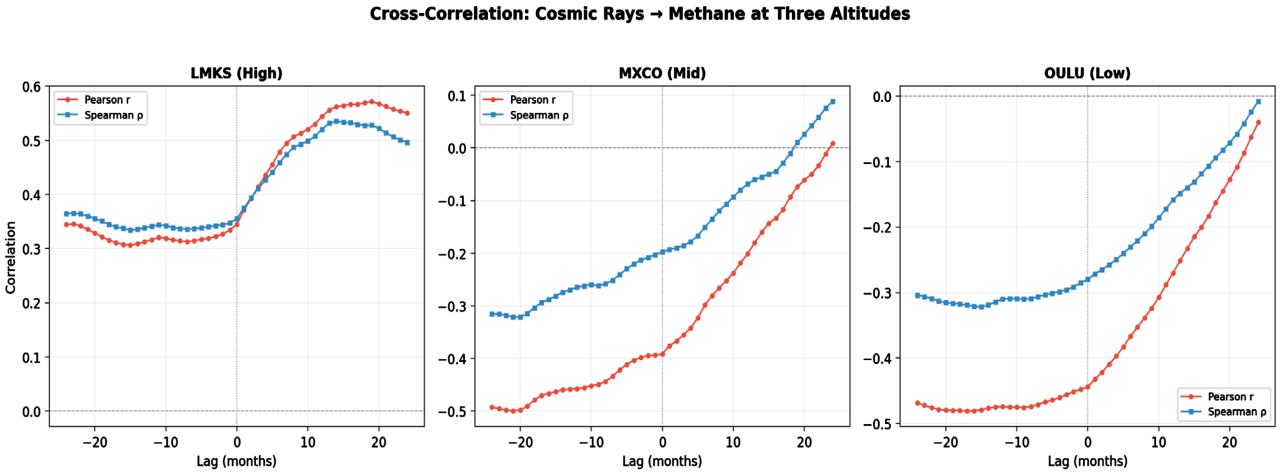

Figure 5. Cross-correlation functions for all three stations. Negative lags indicate GCR leading methane. MXCO peaks at −21 months, OULU at −17 months, and LMKS at +19 months (explanatory).

The LMKS lag profile is qualitatively different. Its peak occurs at +19 months ($r = +0.572$, $p < 10^{-17}$), with the positive lag meaning methane *leads* LMKS cosmic rays by 19 months rather than the reverse. This is physically implausible as a causal mechanism and instead reflects the auto-correlation structure of both trending time series, further confirming that the LMKS-methane relationship is a statistical artefact.

3.5. Limitations

Several limitations should be acknowledged.

1) Correlation does not imply causation, and the observed associations may be mediated by confounding variables not included in this analysis, such as solar UV flux, geomagnetic activity, or stratospheric ozone variability.

2) The study uses global average methane data, which aggregates regional sources and sinks; a regionally disaggregated analysis might reveal clearer cosmic ray-methane signatures.

3) The lag-correlation analysis is exploratory and should be interpreted with caution given the effects of autocorrelation on cross-correlation estimates.

4. Discussion

The result of our work reveals that the relationship between galactic cosmic rays (GCRs) and atmospheric methane depends on altitude; however, it also revealed that not all observed correlations reflect genuine physical connections. At high altitude, the LMKS station appeared to show a positive correlation with methane, but this turned out to be a statistical illusion which showed two unrelated long-term trends (rising methane and cyclic cosmic ray variation) happened to move together over the study period, creating a false impression of a relationship. At mid and low altitudes, the MXCO and OULU stations showed negative correlations that are more physically plausible, since higher cosmic ray flux could boost the production of hydroxyl radicals (OH) in the troposphere, which would speed up methane breakdown and lower its concentration [16].

The analysis highlights how critical it is to control for long-term trends when studying cosmic ray-climate relationships. The LMKS correlation collapsed from a moderate positive value to nearly zero once trends were removed, which is an example of trend confounding. OULU's correlation also weakened and lost significance after seasonal removal and autocorrelation correction, suggesting its raw result was substantially inflated. MXCO's negative correlation survived all preprocessing methods (linear detrending and first differencing) and remained significant after both effective-N correction and block bootstrap testing, making it the strongest and most trustworthy evidence for a genuine sub-decadal physical coupling.

Incidentally, these findings feed into the broader scientific debate about whether cosmic rays meaningfully influence Earth's climate. The Svensmark hypothesis proposes that cosmic ray-driven ionization affects cloud formation and planet's radiation balance [18]; while the CERN CLOUD experiment confirmed that such ionization can enhance aerosol nucleation under laboratory conditions [17]. However, the overall effect sizes observed are modest. Even at MXCO, cosmic ray variability explains only about 15% of methane variance. This is consistent with the understanding that anthropogenic emissions may be the dominant driver. A comprehensive work by [6] argued that while the mechanisms are plausible, the magnitude of the effect remains uncertain and likely small relative to other forcing agents.

Finally, the study draws an important methodological lesson from comparing Pearson and Spearman correlation methods. When these two measures diverge substantially in the raw data as shown by the result obtained from MXCO and OULU, it signals that the relationship may be nonlinear, influenced by outliers, or confounded by trends. After detrending, the two measures converged at MXCO, suggesting the true underlying relationship is approximately linear. Thus, we strongly suggest that researchers studying cosmic ray-climate connections should

routinely report both parametric and non-parametric correlations and always perform detrended analysis as standard practice.

5. Conclusion

This study found statistically significant relationships between galactic cosmic ray flux and global atmospheric methane across all three neutron monitor stations, but detrending revealed that only MXCO retained a credible anti-correlation (with Pearson and Spearman values converging), while LMKS's positive correlation collapsed to insignificance. In the raw (undetrended) analysis, GCR flux explains up to approximately 20% of methane variance (at OULU). However, after removing long-term trends to isolate sub-decadal covariability, the maximum robust explained variance is approximately 15% (at MXCO), confirming that anthropogenic emissions remain the dominant control on atmospheric methane, with the study underscoring the importance of comparing correlation methods and performing detrended analysis as essential safeguards in solar-climate research.

Conflicts of Interest

The authors declare no conflicts of interest regarding the publication of this paper.

References

[1] Masson-Delmotte, V., Zhai, P., Pirani, A., Connors, S. L., Péan, C., Berger, S., *et al.* (2021). Climate Change 2021: The Physical Science Basis. Contribution of Working Group I to the Sixth Assessment Report of the Intergovernmental Panel on Climate Change, 2391 p. https://www.cambridge.org/core/books/climate-change-2021-the-physical-science-basis/415F29233B8BD19FB55F65E3DC67272B

[2] Gaisser, T.K. (1982) Cosmic Rays and Particle Physics. Cambridge University Press.

[3] Usoskin, I.G., Bazilevskaya, G.A. and Kovaltsov, G.A. (2011) Solar Modulation Parameter for Cosmic Rays since 1936 Reconstructed from Ground-Based Neutron Monitors and Ionization Chambers. *Journal of Geophysical Research: Space Physics*, **116**, A02104. https://doi.org/10.1029/2010ja016105

[4] Potgieter, M. (2013) Solar Modulation of Cosmic Rays. *Living Reviews in Solar Physics*, **10**, Article No. 3. https://doi.org/10.12942/lrsp-2013-3

[5] Simpson, J.A. (2000) The Cosmic Ray Nucleonic Component: The Invention and Scientific Uses of the Neutron Monitor—(Keynote Lecture). *Space Science Reviews*, **93**, 11-32. https://doi.org/10.1023/a:1026567706183

[6] Mironova, I.A., Aplin, K.L., Arnold, F., Bazilevskaya, G.A., Harrison, R.G., Krivolutsky, A.A., *et al.* (2015) Energetic Particle Influence on the Earth's Atmosphere. *Space Science Reviews*, **194**, 1-96. https://doi.org/10.1007/s11214-015-0185-4

[7] Loulergue, L., Schilt, A., Spahni, R., Masson-Delmotte, V., Blunier, T., Lemieux, B., *et al.* (2008) Orbital and Millennial-Scale Features of Atmospheric CH4 over the Past 800,000 Years. *Nature*, **453**, 383-386. https://doi.org/10.1038/nature06950

[8] Lan, X., Dlugokencky, E.J., Mund, J.W., Crotwell, A.M., Crotwell, M.J. and Moglia,

E. (2023) Atmospheric Carbon Dioxide Dry Air Mole Fractions from the NOAA GML Carbon Cycle Cooperative Global Air Sampling Network. https://gml.noaa.gov/ccgg/arc/?id=132

[9] Saunois, M., Stavert, A.R., Poulter, B., Bousquet, P., Canadell, J.G., Jackson, R.B., *et al*. (2019) The Global Methane Budget 2000-2017. *Earth System Science Data*, **12**, 1561-1623. https://doi.org/10.5194/essd-2019-128

[10] Kirschke, S., Bousquet, P., Ciais, P., Saunois, M., Canadell, J.G., Dlugokencky, E.J., *et al*. (2013) Three Decades of Global Methane Sources and Sinks. *Nature Geoscience*, **6**, 813-823. https://doi.org/10.1038/ngeo1955

[11] Levy, H. (1971) Normal Atmosphere: Large Radical and Formaldehyde Concentrations Predicted. *Science*, **173**, 141-143. https://doi.org/10.1126/science.173.3992.141

[12] Lelieveld, J., Gromov, S., Pozzer, A. and Taraborrelli, D. (2016) Global Tropospheric Hydroxyl Distribution, Budget and Reactivity. *Atmospheric Chemistry and Physics*, **16**, 12477-12493. https://doi.org/10.5194/acp-16-12477-2016

[13] Prather, M.J., Holmes, C.D. and Hsu, J. (2012) Reactive Greenhouse Gas Scenarios: Systematic Exploration of Uncertainties and the Role of Atmospheric Chemistry. *Geophysical Research Letters*, **39**, L09803. https://doi.org/10.1029/2012gl051440

[14] Atri, D. and Melott, A.L. (2014) Cosmic Rays and Terrestrial Life: A Brief Review. *Astroparticle Physics*, **53**, 186-190. https://doi.org/10.1016/j.astropartphys.2013.03.001

[15] Bazilevskaya, G.A., Usoskin, I.G., Flückiger, E.O., Harrison, R.G., Desorgher, L., Bütikofer, R., *et al*. (2008) Cosmic Ray Induced Ion Production in the Atmosphere. *Space Science Reviews*, **137**, 149-173. https://doi.org/10.1007/s11214-008-9339-y

[16] Calisto, M., Usoskin, I., Rozanov, E. and Peter, T. (2011) Influence of Galactic Cosmic Rays on Atmospheric Composition and Dynamics. *Atmospheric Chemistry and Physics*, **11**, 4547-4556. https://doi.org/10.5194/acp-11-4547-2011

[17] Kirkby, J., Curtius, J., Almeida, J., Dunne, E., Duplissy, J., Ehrhart, S., *et al*. (2011) Role of Sulphuric Acid, Ammonia and Galactic Cosmic Rays in Atmospheric Aerosol Nucleation. *Nature*, **476**, 429-433. https://doi.org/10.1038/nature10343

[18] Svensmark, H. (2007) Cosmoclimatology: A New Theory Emerges. *Astronomy & Geophysics*, **48**, 1.18-1.24. https://doi.org/10.1111/j.1468-4004.2007.48118.x

[19] Svensmark, H., Enghoff, M.B., Shaviv, N.J. and Svensmark, J. (2017) Increased Ionization Supports Growth of Aerosols into Cloud Condensation Nuclei. *Nature Communications*, **8**, Article No. 2199. https://doi.org/10.1038/s41467-017-02082-2

[20] Jackman, C.H., Marsh, D.R., Kinnison, D.E., Mertens, C.J. and Fleming, E.L. (2016) Atmospheric Changes Caused by Galactic Cosmic Rays over the Period 1960–2010. *Atmospheric Chemistry and Physics*, **16**, 5853-5866. https://doi.org/10.5194/acp-16-5853-2016

[21] Price, C., Penner, J. and Prather, M. (1997) NO_x from Lightning: 1. Global Distribution Based on Lightning Physics. *Journal of Geophysical Research*: *Atmospheres*, **102**, 5929-5941. https://doi.org/10.1029/96jd03504

[22] Pudovkin, M.I. and Raspopov, O.M. (1992) Mechanism of Solar Activity Influence on the Lower Atmosphere and Meteorological Parameters. *PIE Proceedings*, **2111**, 163-179.

[23] Laken, B.A., Pallé, E., Čalogović, J. and Dunne, E.M. (2012) A Cosmic Ray-Climate Link and Cloud Observations. *Journal of Space Weather and Space Climate*, **2**, A18. https://doi.org/10.1051/swsc/2012018

[24] Mavromichalaki, H., Papaioannou, A., Plainaki, C., Sarlanis, C., Souvatzoglou, G., Ger-

ontidou, M., *et al*. (2011) Applications and Usage of the Real-Time Neutron Monitor Database. *Advances in Space Research*, **47**, 2210-2222. https://doi.org/10.1016/j.asr.2010.02.019

[25] Hauke, J. and Kossowski, T. (2011) Comparison of Values of Pearson's and Spearman's Correlation Coefficients on the Same Sets of Data. *QUAGEO*, **30**, 87-93. https://doi.org/10.2478/v10117-011-0021-1

[26] Virtanen, P., Gommers, R., Oliphant, T.E., Haberland, M., Reddy, T., Cournapeau, D., *et al*. (2020) SciPy 1.0: Fundamental Algorithms for Scientific Computing in Python. *Nature Methods*, **17**, 261-272. https://doi.org/10.1038/s41592-019-0686-2

[27] Bretherton, C.S., Widmann, M., Dymnikov, V.P., Wallace, J.M. and Bladé, I. (1999) The Effective Number of Spatial Degrees of Freedom of a Time-Varying Field. *Journal of Climate*, **12**, 1990-2009. https://doi.org/10.1175/1520-0442(1999)012<1990:tenosd>2.0.co;2